Ion-Mediated Nucleic Acid Helix-Helix Interactions

Zhi-Jie Tan and Shi-Jie Chen
Department of Physics and Astronomy and Department of Biochemistry, University of Missouri, Columbia, Missouri

ABSTRACT Salt ions are essential for the folding of nucleic acids. We use the tightly bound ion (TBI) model, which can account for the correlations and fluctuations for the ions bound to the nucleic acids, to investigate the electrostatic free-energy landscape for two parallel nucleic acid helices in the solution of added salt. The theory is based on realistic atomic structures of the helices. In monovalent salt, the helices are predicted to repel each other. For divalent salt, while the mean-field Poisson-Boltzmann theory predicts only the repulsion, the TBI theory predicts an effective attraction between the helices. The helices are predicted to be stabilized at an interhelix distance ~26–36 Å, and the strength of the attractive force can reach $-0.37\ k_BT$/bp for helix length in the range of 9–12 bp. Both the stable helix-helix distance and the strength of the attraction are strongly dependent on the salt concentration and ion size. With the increase of the salt concentration, the helix-helix attraction becomes stronger and the most stable helix-helix separation distance becomes smaller. For divalent ions, at very high ion concentration, further addition of ions leads to the weakening of the attraction. Smaller ion size causes stronger helix-helix attraction and stabilizes the helices at a shorter distance. In addition, the TBI model shows that a decrease in the solvent dielectric constant would enhance the ion-mediated attraction. The theoretical findings from the TBI theory agree with the experimental measurements on the osmotic pressure of DNA array as well as the results from the computer simulations.

INTRODUCTION

Nucleic acids (DNAs and RNAs) are highly charged polyanionic chain molecules. The folding of nucleic acids requires the cations to neutralize the negative backbone charges. Therefore, the solvent ionic conditions, including salt concentration, ionic charge and size, solvent dielectric constant, and temperature play essential roles in the folding of nucleic acids (1–10).

Despite the extensive experimental and theoretical studies (11–19), our ability to make accurate quantitative predictions for the ion effects on the folding of complex secondary structures is quite limited, especially in multivalent metal ion solutions. Even if the ion-dependence of the secondary structure folding can be accurately predicted, we are still unable to quantitatively understand how ions assist the extended secondary structural segments to fold up into the compact tertiary structures. Experiments have shown that nucleic acid (RNA) folding undergoes a collapse process (20–28), where the secondary structural segments (e.g., helices) approach each other to form a compact state. A rudimentary process in chain collapse is the aggregation of helices. In this study, we investigate how the metal ions assist the folding (aggregation) of two finite-length helices and how the different ionic conditions affect the helix-helix electrostatic interactions. Since helix-helix recognition is a fundamental tertiary interaction in nucleic acids, this study may provide a paradigm for the ion-assisted nucleic acid tertiary interactions.

For RNAs, various experiments have shown that multivalent ions are efficient to cause chain compaction (20–28). Among other forces, the cation-mediated electrostatic helix-helix attraction can be a possible candidate for the driving force to cause the collapse of RNAs (20–22). Experiments have been designed to probe the driving force for RNA collapse in order to shed light on the mechanism of RNA compaction (28,29). In addition, DNAs, which are long polyanionic molecules, need to condense into compact particles in cells. DNA condensation, a process similar to RNA compaction, has been studied for over two decades (30–40). Experimental and theoretical studies suggest that a possible driving force for DNA helix-helix attraction may come from the correlated multivalent cations (30–40). In addition, for other polyelectrolyte molecules, such as F-actin, filamentous viruses fd and M13, and nucleosomes, experiments have shown the similar multivalent ion-induced collapse (aggregation) (41–47).

Parallel to the experimental development, different theories and computational models have been developed to treat the helix-helix electrostatic interaction. There have been primarily two types of polyelectrolyte theories used to treat helix-helix interactions: the Poisson-Boltzmann (PB) theory (48–55) and the counterion condensation (CC) theory (56). Both theories have been very useful in predicting many thermodynamic properties of nucleic acids and proteins in salt solutions. For the helix-helix interaction, however, the PB theory, which ignores the interion correlations, predicts only repulsive force (57). In contrast, the CC theory predicts attractive forces in both monovalent and multivalent ion solutions and the CC theory attributes the attraction to the increased ion entropy (58–61).

Computer simulations have shown that attraction occurs only in the presence of multivalent ions (62–72). Models based on the simplified structures of the helices (in an asymptotically dilute salt solution) suggest that the attraction may arise from the correlated ion configurations on the surface of

---

Submitted March 1, 2006, and accepted for publication April 14, 2006.

Address reprint requests to Shi-Jie Chen, E-mail: chenshi@missouri.edu.

0006-3495/06/07/518/19 $2.00

doi: 10.1529/biophysj.106.084285

the approaching polyelectrolytes (73–82). When two highly charged polyelectrolytes (helices) approach each other, the strong electric field drives the ions between the helices to self-organize in order to lower the total energy. In the low-temperature limit, the strongly correlated ions can form a Wigner crystal-like configuration and the attraction between two polyelectrolytes can be strong. As the temperature is increased, the Wigner crystal-like ion configuration would be disrupted gradually and the strength of attraction decreases. Both experiments (38,46) and computer simulations (63,66, 69,79) have suggested the existence of the correlated states of the ions. However, the simplified models cannot treat detailed helix structure, which can be essential in the quantitative prediction of the interhelix force. In this study, we aim to obtain a detailed microscopic picture for the ion-mediated helix-helix interaction for realistic nucleic acid helix structures.

Recently, we developed a statistical mechanical theory (denoted the tightly bound ion theory, abbreviated as TBI theory) for nucleic acid molecules. An advantage of the theory is that it can explicitly account for the correlations and the fluctuations for bound ions near the molecule surface (83). As tested against experiments, computer simulations, and the PB and the CC theories (83), the TBI theory gives reliable ion-dependent predictions such as the ion dependence of the helix-coil transition for DNA in both NaCl and $MgCl_2$ solutions (84). In this study, we apply the TBI theory to investigate the ion-mediated nucleic acid helix-helix interactions. Compared with the previous simplified models, the present TBI theory (83,84) is based on realistic helical structure at the atomic level and can treat the dependence on the charge, the concentration, and the size of the added salt ions in the supporting solutions. Moreover, the present model can account for the different binding modes of the bound ions and the fluctuations of the binding modes and the electrostatic and excluded volume correlations between the bound ions. The fluctuations and correlations can play significant roles for multivalent ions such as Mg^{2+} ion solution.

In this work, based on the TBI theory, we calculate the electrostatic free energy for two parallel nucleic acid helices of finite length in the presence of monovalent or divalent salt solutions. We investigate how the helix-helix interaction depends on the ion valency, ion size, ion concentration, and solvent dielectric constant. We also analyze the driving force for the ion-mediated helix-helix attraction. In addition, we compare the predictions with the experimental measurements on osmotic pressure of DNA array as well as with Monte Carlo simulations.

THEORY AND METHODS

Tightly bound ions and tightly bound region

The primary motivation to develop the tightly bound ion (TBI) theory is to go beyond the mean-field approach by treating the ion correlation and fluctuation effects for polyelectrolyte systems (83,84). The basic idea is to classify two types of ions according to ion-ion correlation strength: the (strongly correlated) tightly bound ions and the (weakly correlated) diffusively bound ones. Correspondingly, the solution can be divided into two regions: the tightly bound region and the diffusively bound region. The motivation to distinguish the two types of ions is to treat them separately. For the (weakly correlated) diffusively bound ions, we use PB; for the (strongly correlated) tightly bound ions, we use a separate treatment to explicitly account for the ion correlations and fluctuations.

The tightly/diffusively bound regions are determined by the ion-ion correlation condition. We consider 1), the electrostatic correlation, measured by the parameter $\Gamma(\mathbf{r})$,

$$\Gamma(\mathbf{r}) = \frac{(zq)^2}{\epsilon a_{ws}(\mathbf{r}) k_B T}, \tag{1}$$

and 2), the excluded volume correlation, measured by the ion radius r_c and the Wigner-Seitz radius $a_{ws}(\mathbf{r})$ (83,84). In Eq. 1, $\mathbf{r}$ is the position vector, zq is the charge of cations, ϵ is the dielectric constant of solute, and $a_{ws}(\mathbf{r})$ is the Wigner-Seitz radius, which is given by the cation concentration $c(\mathbf{r})$ in excess of the bulk concentration c^0 (73),

$$\frac{4\pi}{3}[a_{ws}(\mathbf{r})]^3[c(\mathbf{r}) - c^0] = 1. \tag{2}$$

The tightly bound region is defined as position $\mathbf{r}$ such that either $\Gamma(\mathbf{r})$ is larger than a critical value Γ_c so the Coulombic correlation is strong, or $a_{ws}(\mathbf{r})$ is smaller than $(r_c + \Delta r)$ so ions are so crowded that they can easily bump into each other (83,84):

$$\Gamma(\mathbf{r}) \geq \Gamma_c; 2a_{ws}(\mathbf{r}) \leq 2(r_c + \Delta r). \tag{3}$$

Here, Δr is the mean displacement of ions deviating from their equilibrium positions, and $2(a_{ws}(\mathbf{r}) - \Delta r)$ is the closest distance of approach between two ions before they overlap.

Equation 3 gives the criteria to characterize the strong Coulombic and excluded volume correlations, respectively. The value Γ_c is chosen to be 2.6, the critical value for the gas-liquid transition point in ionic systems (85–87), and $\Delta r/d \simeq 0.1$ is used as the melting point for the correlated structure according to Lindemann's melting theory (88–90).

As an approximation, we compute $c(\mathbf{r})$ using the nonlinear PB equation

$$\nabla \cdot \epsilon_0 \epsilon \nabla \psi(\mathbf{r}) = -4\pi \left\{ \rho_f + \sum_\alpha z_\alpha q c_\alpha(\mathbf{r}) \right\}; \tag{4}$$

$$c_\alpha(\mathbf{r}) = c_\alpha^0 e^{-z_\alpha q \psi(\mathbf{r})/k_B T}, \tag{5}$$

where α denotes the ion species, $z_\alpha q$ is the charge of the ion, and c_α^0 is the bulk ion concentration. The value ρ_f is the charge density for the fixed charges, ϵ_0 is the permittivity of free space, and $\psi(\mathbf{r})$ is the electrostatic potential at $\mathbf{r}$. From $c(\mathbf{r})$ and Eq. 3, we can unambiguously define the tightly bound region (83,84). In Fig. 1 we show examples of the tightly bound regions around two parallel DNA helices separated at different distances.

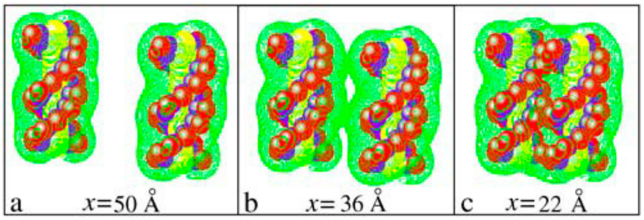

FIGURE 1 The tightly bound regions around two parallel 12-bp B-DNA helices in a divalent ion solution with different interaxis separations: (*a*) 50 Å; (*b*) 36 Å; and (*c*) 22 Å. The divalent salt concentration is 0.1 M and the cation radius is 3.5 Å. The red spheres represent the phosphate groups and the green dots represent the points at the boundaries of the tightly bound regions. The B-DNA helices are produced from the grooved primitive model (83,84,118).